Review

Kinetics of Receptor-Ligand Interactions in Immune Responses

Mian Long[1, 2], Shouqin Lü[1] and Ganyun Sun[1]

Receptor-ligand interactions in blood flow are crucial to initiate the biological processes as inflammatory cascade, platelet thrombosis, as well as tumor metastasis. To mediate cell adhesions, the interacting receptors and ligands must be anchored onto two apposing surfaces of two cells or a cell and a substratum, i.e., the two-dimensional (2D) binding, which is different from the binding of a soluble ligand in fluid phase to a receptor, i.e., three-dimensional (3D) binding. While numerous works have been focused on 3D kinetics of receptor-ligand interactions in immune systems, 2D kinetics and its regulations have less been understood, since no theoretical framework and experimental assays have been established until 1993. Not only does the molecular structure dominate 2D binding kinetics, but the shear force in blood flow also regulates cell adhesions mediated by interacting receptors and ligands. Here we provided the overview of current progresses in 2D bindings and regulations. Relevant issues of theoretical frameworks, experimental measurements, kinetic rates and binding affinities, and force regulations, were discussed. *Cellular & Molecular Immunology*. 2006;3(2):79-86.

Key Words: kinetics, force, receptor-ligand bond, cell adhesion

Introduction

Cell adhesion is a fundamental biological process that is mediated by specific interactions between adhesion receptors and their ligands on other cell surfaces or in extracellular matrix (1, 2). Such adhesions are important to inflammatory cascade, platelet thrombosis, as well as tumor metastasis (3). For example, interactions between selectins and glycol-conjugates mediate leukocyte tethering to and rolling on vascular surfaces at sites of inflammation or injury (4-6). The selectin family of adhesion molecules has three known members: P-, E-, and L-selectin. Their common structure is an N-terminal, C-type lectin (Lec) domain, followed by an epidermal growth factor (EGF)-like module, multiple copies of consensus repeat (CR) units characteristic of complement binding proteins, a transmembrane segment, and a short cytoplasmic domain (7). P-selectin glycoprotein ligand 1 (PSGL-1), as one of major selectin ligands, consists of homo-dimer cross-linked by disulphide bonds, and binds to selectins by its N-terminal peptide which includes three tyrosine sulfates and the core-2 O-glycan (8-12). As another example, circulating immunoglobulin G (IgG) bind to foreign particles or damaged tissue through dual antigen-binding fragments (Fab). The conserved Fc fragment is available for binding by Fcγ receptors (FcγRs) on the immune cell surface, which triggers a wide variety of immune responses (13-15).

Interactions of cellular adhesive molecules are determined by their intrinsic kinetics (reaction rates and binding affinity), since kinetic parameters govern how likely and how fast the adhesion occurs, and how strong and how long the bond remains bound. In a typical 2D binding, at least two specific aspects arise as compared to 3D binding (16). One aspect is the coupling of kinetics and mechanics, so-called mechano-chemical coupling, of receptor-ligand interactions. In blood flow, cell adhesions are regulated by hemodynamic forces which are translated into external forces on interacting molecules. Bond formation and dissociation of interacting adhesive molecules provide the physical linkages between cells. Not only does applied force regulate the lifetime of molecular interactions, just as pressure affects the chemical rates (17-19), but force loading rate also affects the bond strength of molecular interactions (20). For example, the formations of immunological synapse between a T cell and an antigen presenting cell are governed by both 2D binding kinetics of interacting molecule pairs (i.e., T-cell receptor *vs* major histocompatibility molecules, integrin *vs* ligand) and mechanics of cell membrane (i.e., stiffness, rigidity) (21).

Another aspect is the stochastic nature of receptor-ligand interactions. In contrast to 3D binding where thousands of interacting receptors and ligands are involved and molecular

[1]National Microgravity Laboratory and Center for Biomechanics and Bioengineering, Institute of Mechanics, Chinese Academy of Sciences, Beijing 100080, China;

[2]Corresponding to: Dr. Mian Long, National Microgravity Laboratory and Center for Biomechanics and Bioengineering, Institute of Mechanics, Chinese Academy of Sciences, Beijing 100080, China. Tel: +86-10-6261-3540, Fax: +86-10-6261-3540, E-mail: mlong@imech.ac.cn.

Received Apr 5, 2006. Accepted Apr 16, 2006.

fluctuation of individual molecules is averaged out by their statistical behaviors, molecular bonds in 2D binding are rarely formed inside the contact area. This infrequent occurrence of adhesions introduces the stochastic nature of individual molecules. For example, there are only single or a few bonds of P-selectin-ligand bonds involved in leukocyte-endothelium interactions (22). Moreover, number of bonds varies with time to time. Taken together, these aspects suggest that new theoretical models and experimental measurements are required to understand quantitatively 2D kinetics of receptor-ligand interactions.

In this review, we provided the overview of the current progresses in quantitative understanding of 2D kinetics and forced dissociation of receptor-ligand bindings. Four issues were discussed, including theoretical bases, experimental measurements, 2D kinetics and affinities, and force regulations. These provide new insights into understanding the receptor-ligand interactions in immune responses.

Theoretical framework for receptor-ligand kinetics

Consider a second-order forward and first-order reverse reaction,

$$R + L \underset{k_r}{\overset{k_f}{\rightleftharpoons}} B \tag{1}$$

where R, L, and B denote respectively the receptor, ligand, and bond. In 3D binding, kinetics of a soluble ligand binding to a receptor follows a simple, deterministic kinetic equation,

$$d[B]/dt = k_f[R][L] - k_r[B] \tag{2}$$

where $[R]$, $[L]$, and $[B]$ denote the concentrations of receptor, ligand, and bond respectively (in unit of M), and k_f (in unit of $M^{-1}\cdot s^{-1}$) and k_r (in unit of s^{-1}) are the forward and reverse rates respectively. K_a (= k_f/k_r) is the binding affinity (in unit of M^{-1}) when the reaction reaches an equilibrium state.

2D binding of receptor-ligand interactions in cell-cell or cell-substrate adhesions is a stochastic process regulated by applied forces. On one hand, the stochastic nature of such a binding can be described using a probabilistic model. The basic idea is to define the probability of bonds, instead of concentration of bonds, since the adhesion is no longer a deterministic process. Upon a small system kinetics first proposed by McQuarrie (23), a probabilistic modeling has been developed and the adhesion probability, P_a, at contact time t follows (24-30),

$$P_a = 1 - \exp\left\{-A_c m_r m_l K_a^0 \left[1 - \exp\left(-k_r^0 t\right)\right]\right\} \tag{3}$$

where K_a^0 (in unit of μm^2) and k_r^0 are respectively the zero-force binding affinity and reverse rate, m_r and m_l are respectively the site densities of receptor and ligand (in unit of μm^{-2}), and A_c is the contact area (in unit of μm^2). 2D kinetic parameters of $A_c m_l K_a^0$ (if m_r is known) or $A_c K_a^0$ (if both m_r and m_l are known) and k_r^0 can be predicted by fitting the experimental measurements of binding curves ($P_a \sim t$ curves) to the model (Eq. 3), and 2D forward rate k_f (in unit of $\mu m^2\cdot s^{-1}$) can be obtained by the definition (= $K_a^0 \times k_r^0$).

On the other hand, force regulates the formation and dissociation of bonds in blood flow. Two parameters are used to quantify the effect: one is the bond rupture force or bond strength, and the other is bond lifetime. Bond rupture force depends on the rate of force application, or force loading rate (20, 31-40), and other extrinsic physical parameters (41). Bond lifetime is governed by external forces, as proposed by Bell (17) and Dembo (18),

$$k_r = k_r^0 \exp\left(\pm \frac{af}{k_B T}\right) \tag{4}$$

where k_r is the reverse rate at force f, a is the interaction range, and k_B and T are respectively the Boltzmann constant and absolute temperature. Noting that the bond lifetime, τ, is the reciprocal of reverse rate ($\tau = 1/k_r$) at any given force, f, Eq. 4 gives out two mechanisms of forced dissociation of bonds: bond lifetime τ decreases with f (if positive symbol is given in Eq. 4) which is termed as *slip bond* (17, 42-45), or increases with f (if negative symbol is given in Eq. 4) which is termed as *catch bond* (18, 46-49). Experimental measurements of bond lifetime at systematically varied forces can be used to determine the force dependence of bond lifetime, which is used to test the theoretical predictions (Eq. 4).

Experimental assays in measuring 2D kinetics

Until 1993, 2D kinetics measurements have not been available experimentally (50). From that on, many experimental assays have been developed by coordinating the biological experiments and mechanical measurements. These include micropipette aspiration (24-29), optical tweezer (30, 31), biological force probe (32-34), atomic force microscopy (AFM) (35-40, 46, 47), flow chamber (42-45, 50), micro-cantilever needle (51), centrifugation (52), rosetting (53-55), cone-plate viscometer (56-58), surface force apparatus (59, 60), and fluorescence recovery after photobleaching (FRAP) (61, 62). Here two assays of micropipette aspiration and atomic force microscopy are reported to demonstrate how the assays work.

In a micropipette aspiration assay, two cells (generally a human red blood cell (RBC) and a nucleated cell respectively expressing or coated with a receptor and the counterpart ligand) are respectively aspirated by two micropipettes with diameters of ~1.5-3 μm *via* a suction pressure of 1-4 mmH_2O (24-29) (Figure 1a). Adhesion between the RBC and the nucleated cell is staged by placing them onto controlled contact *via* micromanipulation (Figure 1b). The presence of adhesion and the adhesion force at the end of a given contact period are detected mechanically by observing microscopically the deflection of the flexible RBC membrane upon retracting it away from the nucleated cell (Figures 1c and 1d). This contact-retraction cycle is repeated one hundred times to estimate the adhesion probability, P_a, at that contact duration, t. ~100 pairs of cells are used to obtain several P_a *vs* t curves that correspond to different receptor and ligand densities, m_r and m_l. Eq. 3 is used to estimate the zero-force reverse rate,

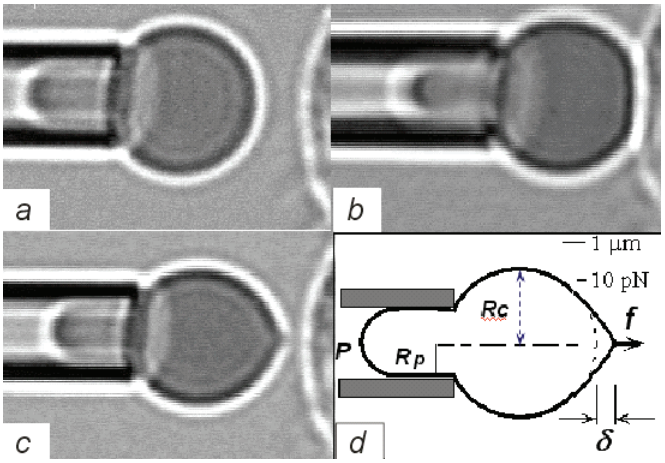

Figure 1. **Micropipette aspiration assay.** (a) A P-selectin-coated RBC (left) and a PSGL-1-expressing HL-60 cell (right; partially shown) are aspirated by a respective micropipette. (b) RBC is brought into contact with HL-60 cell with controlled contact area and given contact duration by piezoelectric translator. (c) Adhesion between two cells is mechanically detected by observing the deformation of RBC apex when it is retracted away from HL-60 cell. (d) Adhesion force f between two cells is estimated to be the product of deflection, δ, and stiffness of RBC (80).

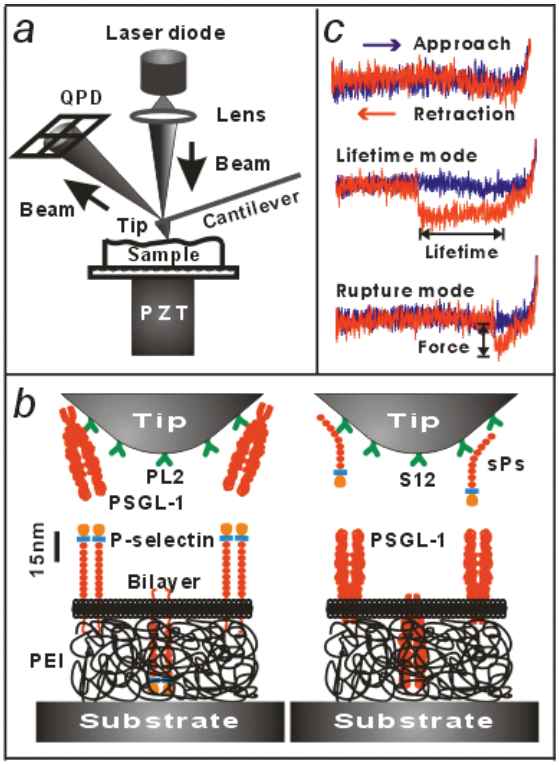

Figure 2. **Atomic force microscopy assay.** (a) A piezoelectric translator is used to drive the movement of stage and to bring the interacting molecules into contact. Adhesion and force signals are collected from a quad photodetector, which measures the laser reflected on the back of the cantilever. (b) Soluble P-selectin was captured by its non-blocking mAb S12 pre-adsorbed on the AFM tip. Purified native PSGL-1 was reconstituted in a lipid bilayer supported by a PEI-cushioned substrate (right panel). A reversely conformational system is also shown (left panel). (c) Interacting molecules are driven to approach to (from left to right, blue line), contact with, and retract from (from right to left, red line) each other, and adhesion is visualized from the cantilever deflection. Bond lifetime is measured from force-time curve (middle panel), and rupture force is measured from force-displacement curve (lower panel).

k_r^0, and effective binding affinity, $A_c m_l K_a^0$ (if m_r was known) or $A_c K_a^0$ (if both m_r and m_l were known).

In an atomic force microscopy assay, a receptor or ligand is coated directly or captured *via* capturing monoclonal antibody (mAb) onto AFM cantilever tip. Purified counter-part ligands or receptors are incorporated in lipid vesicles and then reconstituted by vesicle fusion in a polyethylenimine (PEI) polymer-supported lipid bilayer onto mica or glass surface before use (Figure 2b) (38, 41, 46, 47). The ligand- or receptor-reconstituted lipid bilayer is placed on the AFM stage, which is repeatedly driven to approach the receptor- or ligand-coated cantilever tip, to make contact to allow reversible bond formation and dissociation, and to retract away to allow observation of the adhesion event and measurement of lifetime or rupture force, if any (Figure 2c). The adhesion and lifetime or force signals for each approach-contact-retract cycle are collected from a quad photodetector (Figure 2a). Different locations on each lipid bilayer are tested for 150-400 cycles at each location to collect a set of adhesion events and lifetimes or rupture forces, and all experiments are repeated using a set of different lipid bilayers. Measured P_a *vs* t data is fitted to the model (Eq. 3) to obtain the kinetic parameters (k_r^0 and $A_c m_r m_l K_a^0$) (41). Bond lifetime data, $<\tau>$ *vs* f, are measured to test the forced-dissociation hypotheses (Eq. 4) (46, 47), and bond rupture forces are measured at given force loading rates (38, 41).

It should be pointed out that slight differences might exist in determining quantitatively kinetic parameters, bond rupture force, and bond lifetime when different assays are used for same molecular system. This should not be surprising since experimental conditions are hardly to be kept identical from one assay to another. Nevertheless, these assays provide the new insight into quantifying the binding kinetics and force dependence of dissociation of receptor-ligand interactions.

2D kinetics is determinant to receptor-ligand recognition

One biological issue for 2D binding of receptor-ligand interactions is how molecular structures determine the functionality of cell adhesions. Different species of ligands bind to their receptors with varied kinetic rates and affinities. For example, E-selectin dissociates 2-fold faster from HL-60 cells expressing PSGL-1 than Colo-205 cells expressing both

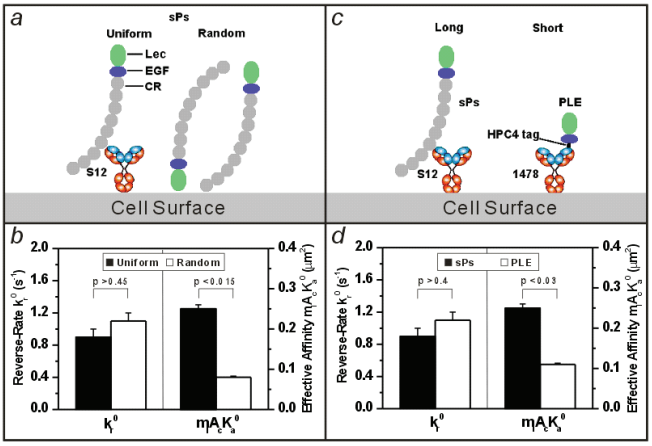

Figure 3. **Surface presentation influences the 2D forward rates but not the reverse rates.** (a, c) P-selectin is uniformly oriented by capturing *via* its capturing mAb S12 or randomly oriented by directly coating *via* $CrCl_3$ coupling (a), or long (sPs) or short (P-LE) P-selectin is coupled by directly coating *via* $CrCl_3$ coupling on RBC surface (c). (b, d) Kinetic parameters of reverse rates, k_r^0, and effective binding affinities, $m_\mu A_c K_a^0$, are compared in different cases of surface presentations. Data are presented as mean ± SD. *p* value indicates the level of statistical significance of differences in parameters corresponding to the two orientations or to the two lengths.

PSGL-1 and sLe^x carbohydrates (27). CD16A (FcγRIII) binds to rabbit IgG with 4-fold higher affinity than human IgG (24). Even with same species, different isoforms or constructs of interacting receptors reports distinct binding mechanisms to their ligands. For example, glycosylphosphatidylinositol-anchored CD16A binds faster and with higher affinities to human and rabbit IgGs but slower and with lower affinity to murine IgG2a as compared to transmembrane-anchored CD16A (26). L- or P-selectin transfected preB cells roll more irregularly on and dissociate faster from the substrate of immobilized single tyrosine replacement of PSGL-1 than wild-type PSGL-1 molecules (63). Under static conditions, PSGL-1-expressing neutrophils adhere equivalently to cells expressing wild-type P-selectin that contains 9 CRs units and to P-selectin constructs with as few as two CRs. However, P-selectin requires at least 5 CRs to mediate optimal rolling of flowing neutrophils under shear conditions (64).

Surface presentation of interacting receptors affects the 2D kinetics of receptor-ligand interactions. One surface environmental factor is the orientation of the binding pockets of adhesion receptors. For example, randomizing the orientation of selectin or rabbit IgG lowers 2D affinities of selectin *vs* PSGL-1 or rabbit IgG *vs* CD16A interactions by reducing the forward rates but not the reverse rates (Figures 3a and 3b). In contrast, the soluble antibody binds with similar three-dimensional affinities to cell-bound P-selectin constructs regardless of their orientation (28). HL-60 cells adhere to short E-selectin constructs with two or less CRs when they are captured by a nonblocking monoclonal antibody adsorbed on the plastic surface (65). Cell adhesion to fibronectin is regulated by surface chemistries that alter fibronectin adsorption (66). Cells expressing an L-selectin construct that replaces its EGF domain with the EGF domain of P-selectin roll better on L-selectin ligands than cells expressing wild-type L-selectin, probably because an altered orientation of Lec domain enhances the association rate with surface ligands (67). Another surface environmental factor is the length of the binding pockets above the cell membrane. For example, lowering selectin ligand- and antibody-binding domain above the cell membrane lowers 2D affinities of selectin *vs* PSGL-1 or rabbit IgG *vs* CD16A interactions by reducing the forward rates but not the reverse rates (Figures 3c and 3d). In contrast, the soluble antibody binds with similar three-dimensional affinities to cell-bound P-selectin constructs regardless of their length (28). Extending the binding site of CD58 above the cell membrane in the stalk (~15 nm) enhances its binding to CD2 on T lymphocytes (68). K562 cells bearing a glycosulfopeptide 2-GSP-6 modeled after the binding domain of PSGL-1, which is attached to the membrane-distal region of a nonbinding molecule ~50 nm above the cell surface, roll more stably on P-selectin than cells bearing 2-GSP-6 randomly attached to cell surface proteins (69). HL-60 cells bind to immobilized full-length E-selectin that contains all six CRs but not to shorter E-selectin constructs with two or less CRs (65).

Membrane microtopology and cell deformation onto which the interacting receptors are anchored also influence the 2D receptor-ligand kinetics. For example, Fcγ receptor CD16B binds to IgG with a 50-fold higher in effective 2D affinity A_cK_a for receptors anchored on smooth RBCs than those on rough CHO and K562 cells, whereas the reverse rates are similar for all three (29). Rough cells may initially mediate the point contact, whereas smooth cells initiate the area contact, which results in the differences in contact area A_c. As of another example, PSGL-1 localized on the tips of elastic microvilli slows neutrophils rolling on P-selectin substrate and lowers reverse rate, as compared to PSGL-1 coupled onto rigid polystyrene microbeads. However, fixed neutrophils with less deformation support relatively faster rolling and dissociation than resting neutrophils (70).

Force affects the receptor-ligand interactions

Another issue of 2D kinetics of receptor-ligand interactions is that applied forces regulate the dissociation of receptor-ligand bonds. Under physiological conditions, blood flow exerts shear forces on cells that must be balanced by adhesive forces on receptor-ligand bonds, which regulates their formations and dissociations. This is very different from 3D binding in blood flow where no forces are exerted on the bonds in a fluid phase. For example, selectin-ligand binding has served as a model system for the first intensive analysis of how reverse rates depend on force (31, 33-37, 41-47) and on the history of force application (38). When a ramp force is applied to break the bond, the force dependence of reverse rate translates to the dependence of rupture force on force

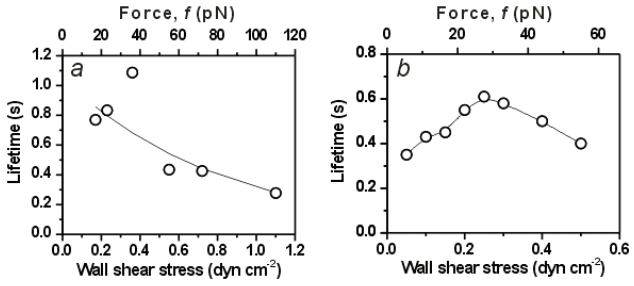

Figure 4. Forces regulate the dissociations of receptor-ligand bonds. (a) Bond lifetime of P-selectin-PSGL-1 interactions decreases with corresponding intermolecular force (*slip bond*) (Adopted from (42)). (b) Bond lifetime of P-selectin-PSGL-1 interactions increases at lower forces and decreases at higher forces with corresponding intermolecular force (*catch-slip bond transition*) (Adopted from (46)). Experiments were performed by PSGL-1 expressing neutrophil tethering onto P-selectin absorbed substrate using a flow chamber assay.

loading rate (31, 33-38, 41). The theory of dynamic force spectroscopy predicts that the bond strength, defined as the most probable rupture force, increases linearly with the logarithm of loading rate (20, 31, 33-38, 41).

Force regulation of reverse rate for dissociation of receptor-ligand bonds has been extensively studied. There is a growing body of evidence supporting that bond lifetime is shortened with forces in a wide and relatively high force range，i.e., slip bond (Figure 4a) (42-45). Recently, P- and L-selectin have been shown to form catch bonds at low forces, and slip bonds at high forces with PSGL-1, as exemplified in Figure 4b (46, 47). To explain transitions between catch and slip bonds, a two-pathway model has been proposed, which assumes the existence of two bound states that dissociate along two pathways with distinct sensitivity to force (34, 71). The potential presence of dual bound states may provide a possible mechanism for the velocity for the interacting molecules to approach each other to regulate the bond strength by biasing the proportions of the two bound states. It may also interpret the "shear threshold" phenomena of dissociation of L-selectin-ligand bonds (72, 73).

Other extrinsic physical factors also govern selectin-ligand interactions that mediate tethering and rolling of circulating cells on the vessel wall under hemodynamic forces. There exists, in a typical AFM study on forced dissociation of P-selectin-PSGL-1 bonds, a saturable relationship between the contact time and the rupture force, a biphasic relationship between the adhesion probability and the retraction velocity, and a threshold relationship between the approach velocity and the rupture force (41). Microbeads bearing PSGL-1 or fixed neutrophils roll faster over P-selectin-coated substrate and have higher reverse rates of bond dissociations than native neutrophils (69).

Molecular conformations provide structural bases to forced dissociations of receptor-ligand bonds. Steered molecular dynamics (SMD) simulation, a well-developed numerical approach which conducts the simulations of

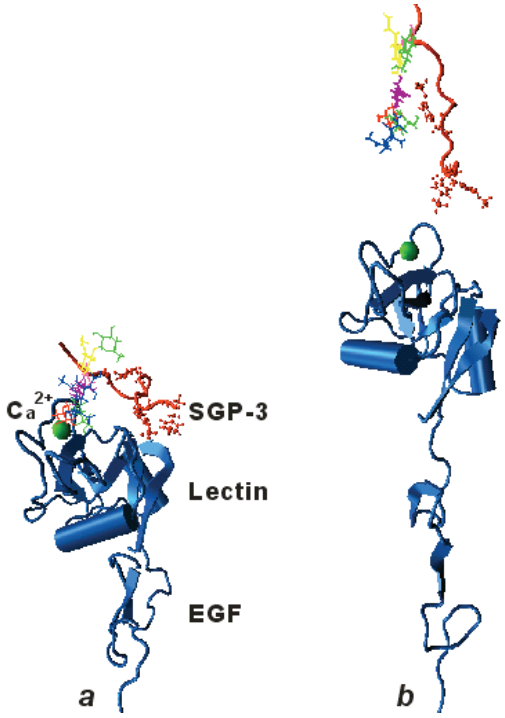

Figure 5. Conformation of P-LE-SGP-3 complex evolves during forced dissociation using SMD simulations, where P-LE consists of Lec and EGF domains of P-selectin, and SGP-3 is a synthesized sulfoglycopeptie which is identical to 19 N-terminal amino acids of mature PSGL-1. (a) Initial conformation before forced dissociation. (b) End conformation after forced dissociation at 10 pN/ps of force loading rate. Data are adopted from (79).

force-induced molecule unfolding and complex dissociation and provides the time-dependent conformational evolutions at atomic level, has been widely used in studying the mechanisms of forced protein unfolding (74, 75) and of unbinding of biomolecular complex under applied forces (76-78). For example, intramolecular unraveling in P-LE-SGP-3 complex, the smallest functional unit of P-selectin-PSGL-1 bond, under applied forces mainly resulted from the destroy of two anti-parallel β sheets of EGF domain and the breakage of hydrogen-bond cluster at the Lec-EGF interface of P-selectin, accompanied with intermolecular dissociation of separation of fucose from Ca^{2+} ion (Figure 5). Conformational changes during forced dissociations depended on pulling velocities and forces, as well as on how the force was applied (79).

Summary

Quantifying 2D kinetics and forced dissociations of receptor-ligand interactions in cell adhesions is crucial to further the understandings in immune responses. A probabilistic model of small system is developed to predict 2D kinetic rates and binding affinities, while a chemical-mechanical coupling model is introduced to analyze forced

regulation of receptor-ligand interactions. The state-of-the-art techniques including micropipette aspiration and atomic force microscopy have been used to measure the receptor-ligand binding kinetics and regulation of applied forces. Structural variation, surface environment, and membrane microtopology and stiffness affect the kinetic rates and affinities. Applied forces regulate the bond strength and lifetime in multiple phases.

Acknowledgements

This work was supported by NSFC grants 10332060 and 30225027, and CAS grants KJCX2-SW-L06 and 2005-1-16.

References

1. Springer TA. Traffic signals for lymphocyte recirculation and leukocyte emigration: the multi-step paradigm. Cell. 1994;76: 301-314.
2. Hynes RO. Integrins: bidirectional, allosteric signaling machines. Cell. 2002;110:673-687.
3. McEver RP. Adhesive interactions of leukocytes, platelets, and the vessel wall during hemostasis and inflammation. Thromb Haemost. 2001;86:746-756.
4. Vestweber D, Blanks JE. Mechanisms that regulate the function of the selectins and their ligands. Physiol Rev. 1999;79:181-213.
5. McEver RP. Selectins: lectins that initiate cell adhesion under flow. Curr Opin Cell Biol. 2002;14:581-586.
6. Ley K. The role of selectins in inflammation and disease. Trends Mol Med. 2003;9:263-268.
7. McEver RP. Selectins. Curr Opin Immunol. 1994;6:75-84.
8. Moore KL, Stults NL, Diaz S, et al. Identification of a specific glycoprotein ligand for P-selectin (CD62) on myeloid cells. J Cell Biol. 1992;118:445-456.
9. Li F, Erickson HP, James JA, Moore KL, Cummings RD, McEver RP. Visualization of P-selectin glycoprotein ligand-1 as a highly extended molecule and mapping of protein epitopes for monoclonal antibodies. J Biol Chem. 1996;271:6342-6348.
10. Leppänen A, Mehta P, Ouyang YB, et al. Novel glycosulfopeptide binds to P-selectin and inhibits leukocyte adhesion to P-selectin. J Biol Chem. 1999;274:24838-24848.
11. Epperson TK, Patel KD, McEver RP, Cummings RD. Noncovalent association of P-selectin glycoprotein ligand-1 and minimal determinants for binding to P-selectin. J Biol Chem. 2000;275:7839-7853.
12. Leppänen A, Yago T, Otto VI, McEver RP, Cummings RD. Model glycosulfopeptides from P-selectin glycoprotein ligand-1 require tyrosine sulfation and a core-2-branched O-glycan to bind to L-selectin. J Biol Chem. 2003;278:26391-26400.
13. Unkeless JC, Scigliano E, Freedman VH. Structure and function of human and murine receptors for IgG. Annu Rev Immunol. 1988;6:251-281.
14. Daëron M. Fc receptor biology. Annu Rev Immunol. 1997;15: 203-234.
15. van de Winkel JGJ, Capel PJA. Human IgG Fc receptor heterogeneity: molecular aspects and clinical implications. Immunol Today. 1993;14:215-221.
16. Dustin ML, Bromley SK, Davis MM, Zhu C. Identification of self through two-dimensional chemistry and synapses. Annu Rev Cell Dev. Biol. 2001;17:133-157.
17. Bell GI. Models for the specific adhesion of cells to cells. Science. 1978;200:618-627.
18. Dembo M, Torney DC, Saxman K, Hammer D. The reaction limited kinetics of membrane-to-surface adhesion and detachment. Proc Royal Soc Lond B Biol Sci. 1988;234:55-83.
19. Bruinsma R. Les liaisons dangereuses: adhesion molecules do it statistically. Proc Natl Acad Sci U S A. 1997;94:375-376.
20. Evans E, Ritchie K. Dynamic strength of molecular adhesion bonds. Biophys J. 1997;74:1541-1555.
21. Lee SJE, Hori Y, Groves JT, Dustin ML, Chakraborty AK. Correlation of a dynamic model for immunological synapse formation with effector functions: two pathways to synapse formation. Trends Immunol. 2002;23:492-499.
22. Caputo KE, Hammer DA. Effect of microvillus deformability on leukocyte adhesion explored using adhesive dynamics simulations. Biophys J. 2005;89:187-200.
23. McQuarrie DA. Kinetics of small systems. J Chem Phys. 1963; 38:433-436.
24. Chesla SE, Selvaraj P, Zhu C. Measuring two-dimensional receptor-ligand binding kinetics by micropipette. Biophys J. 1998;75:1553-1572.
25. Williams TE, Selvaraj P, Zhu C. Concurrent binding to multiple ligands: kinetic rates of CD16b for member-bound IgG1 and IgG2. Biophys J. 2000;79:1858-1866.
26. Chesla SE, Li P, Nagarajan S, Selvaraj P, Zhu C. The membrane anchor influences ligand binding two-dimensional kinetic rates and three-dimensional affinity of FcγRIII (CD16). J Biol Chem. 2000;275:10235-10246.
27. Long M, Zhao H, Huang KS, Zhu C. Kinetic measurements of cell surface E-selectin/carbohydrate ligand interactions. Annu Biomed Eng. 2001;29:935-946.
28. Huang J, Chen J, Chesla SE, et al. Quantifying the effects of molecular orientation and length on two-dimensional receptor-ligand binding kinetics. J Biol Chem. 2004;279:44915-44923.
29. Williams TE, Nagarajan S, Selvaraj P, Zhu C. Quantifying the impact of membrane microtopology on effective two-dimensional affinity. J Biol Chem. 2001;276:13283-13288.
30. Thoumine O, Kocian P, Kottelat A, Meister JJ. Short-term binding of fibroblasts to fibronectin: optical tweezers experiments and probabilistic analysis. Eur Biophys J. 2000;29: 398-408.
31. Rinko LJ, Lawrence MB, Guilford WH. The molecular mechanics of P- and L-selectin Lectin domains binding to PSGL-1. Biophys J. 2004;86:544-554.
32. Merkel R, Nassoy P, Leung A, Ritchie K, Evans E. Energy landscapes of receptor-ligand bonds explored with dynamic force spectroscopy. Nature. 1999;397:50-53.
33. Evans E, Leung A, Hammer D, Simon S. Chemically distinct transition states govern rapid dissociation of single L-selectin bonds under force. Proc Natl Acad Sci U S A. 2001;98:3784-3789.
34. Evans E, Leung A, Heinrich V, Zhu C. Mechanical switching and coupling between two dissociation pathways in a P-selectin adhesion bond. Proc Natl Acad Sci U S A. 2004;101:11281-11286.
35. Fritz J, Katopodis AG, Kolbinger F, Anselmetti D. Force-mediated kinetics of single P-selectin/ligand complexes observed by atomic force microscopy. Proc Natl Acad Sci U S A. 1998;95:12283-12288.
36. Hanley W, McCarty O, Jadhav S, Tseng Y, Wirtz D, Konstantopoulos K. Single molecule characterization of P-selectin/ligand binding. J Biol Chem. 2003;278:10556-10561.
37. Zhang XH, Bogorin DF, Moy VT. Molecular basis of the dynamic strength of the sialyl Lewis X-selectin interaction. Chem Phys Chem. 2004;5:175-182.

38. Marshall BT, Sarangapani KK, Lou JZ, McEver RP, Zhu C. Force history dependence of receptor-ligand dissociation. Biophys J. 2005;88:1458-1466.
39. Ros R, Schwesinger F, Anselmetti D, et al. Antigen binding forces of individually addressed single-chain Fv antibody molecules. Proc Natl Acad Sci U S A. 1998;95:7402-7405.
40. Baumgartner W, Hinterdorfer P, Ness W, et al. Cadherin interaction probed by atomic force microscopy. Proc Natl Acad Sci U S A. 2000;97:4005-4010.
41. Lü SQ, Ye ZY, Zhu C, Long M. Quantifying the effects of contact duration, loading rate, and approach velocity on P-selectin-PSGL-1 interactions using AFM. Polymer. 2006;47: 2539-2547.
42. Alon R, Hammer DA, Springer TA. Lifetime of the P-selectin-carbohydrate bond and its response to tensile force in hydrodynamic flow. Nature. 1995;374:539-542.
43. Alon R, Chen S, Puri KD, Finger EB, Springer TA. The kinetics of L-selectin tethers and the mechanics of selectin-mediated rolling. J Cell Biol. 1997;138:1169-1180.
44. Chen S, Springer TA. An automatic braking system that stabilizes leukocyte rolling by an increase in selectin bond number with shear. J Cell Biol. 1999;144:185-200.
45. Chen S, Spinger TA. Selectin receptor-ligand bonds: formation limited by shear rate and dissociation governed by the Bell model. Proc Natl Acad Sci U S A. 2001;98:950-955.
46. Marshall BT, Long M, Piper JW, Yago T, McEver RP, Zhu C. Direct observation of catch bonds. Nature. 2003;423:190-193.
47. Sarangapani KK, Yago T, Klopocki AG, et al. Low force decelerates L-selectin dissociation from P-selectin glycoprotein ligand-1 and endoglycan. J Biol Chem. 2004;279:2291-2298.
48. Forero M, Thomas WE, Bland C, Nilsson LM, Sokurenko EV, Vogel V. A catch-bond based nanoadhesive sensitive to shear stress. Nano Lett. 2004;4:1593-1597.
49. Thomas WE, Nilsson LM, Forefo M, Sokurenko EV, Vogel V. Shear-dependent 'stick-and-roll' adhesion of type 1 fimbriated *Escherichia coli*. Mol Microbiol. 2004;53:1545-1557.
50. Kaplanski G, Farnarier C, Tissot O. Granulocyte endothelium initial adhesion: analysis of transient binding events mediated by E-selectin in a laminar shear flow. Biophys J. 1993;64:1922-1933.
51. Tees DFJ, Waugh RE, Hammer DA. A microcantilever device to assess the effect of force on the lifetime of selectin-carbohydrate bonds. Biophys J. 2001;80:668-682.
52. Piper JW, Swerlick RA, Zhu C. Determining the force dependence of two dimensional receptor-ligand binding affinity by centrifugation. Biophys J. 1998;74:492-513.
53. Selvaraj P, Plunkett ML, Dustin ML, Sanders ME, Shaw S, Springer TA. The T-lymphocyte glycoprotein CD2 binds the cell surface ligand LFA-3. Nature. 1987;326:400-403.
54. Selvaraj P, Dustin ML, Mitnacht R, Hunig T, Springer TA, Plunkett ML. Rosetting of human T lymphocytes with sheep and human erythrocytes. Comparison of human and sheep ligand binding using purified E receptor. J Immunol. 1987;139: 2690-2695.
55. Long M, Chen J, Jiang N, Selvaraj P, McEver RP, Zhu C. Probabilistic modeling of rosette formation. Biophys J. 2006; in press.
56. Tees DFJ, Coenen O, Goldsmith HL. Interaction forces between red cells agglutinated by antibody. IV. Time and force dependence of break-up. Biophys J. 1993;65:1318-1334.
57. Tees DFJ, Goldsmith HL. Kinetics and locus of failure of receptor-ligand-mediated adhesion between latex spheres. I. protein-carbohydrate bond. Biophys J. 1996;71:1102-1114.
58. Long M, Goldsmith HL, Tees DFJ, Zhu C. Probabilistic modeling of shear-induced formation and breakage of doublets cross-linked by receptor-ligand bonds. Biophys J. 1999;76: 1112-1128.
59. Leckband D. The surface force apparatus - a tool for probing molecular protein interactions. Nature. 1995;376:617-618.
60. Sridhar I, Johnson KL, Fleck NA. Adhesion mechanics of the surface force apparatus. J Phys D: Appl Phys. 1997;30:1710-1719.
61. Meyvis TKL, De Smedt SC, Van Oostveldt P, Demeester J. Fluorescence recovery after photobleaching: a versatile tool for mobility and interaction measurements in pharmaceutical research. Pharm Res. 1999;16:1153-1162.
62. Triantafilou K, Triantafilou M, Ladha S, et al. Fluorescence recovery after photobleaching reveals that LPS rapidly transfers from CD14 to hsp70 and hsp90 on the cell membrane. J Cell Sci. 2001;114:2535-2545.
63. Ramachandran V, Nollert MU, Qiu H, et al. Tyrosine replacement in P-selectin glycoprotein ligand-1 affects distinct kinetic and mechanical properties of bonds with P- and L-selectin. Proc Natl Acad Sci U S A. 1999;96:13771-13776.
64. Patel KD, Nollert MU, McEver RP. P-selectin must extend a sufficient length from the plasma membrane to mediate rolling of neutrophils. J Cell Biol. 1995;131:1893-1902.
65. Lis SH, Burns DK, Rumberger JM, et al. Consensus repeat domains of E-selectin enhance ligand binding. J Biol Chem. 1994;269:4431-4437.
66. Michael KE, Vernekar VN, Keselowsky BG, Meredith JC, Latour RA, Garcia AJ. Adsorption-induced conformational changes in fibronectin due to interactions with well-defined surface chemistries. Langmuir. 2003;19:8033-8040.
67. Dwir O, Kansas GS, Alon R. An activated L-selectin mutant with conserved equilibrium binding properties but enhanced ligand recognition under shear flow. J Biol Chem. 2000;275: 18682-18691.
68. Chan PY, Springer TA. Effect of lengthening lymphocyte function-associated antigen 3 on adhesion to CD2. Mol Biol Cell. 1992;3:157-166.
69. Yago T, Leppänen A, Qiu H, et al. Distinct molecular and cellular contributions to stabilizing selectin-mediated rolling under flow. J Cell Biol. 2002;158:787-799.
70. Park EYH, Smith MJ, Stropp ES, et al. Comparison of PSGL-1 microbead and neutrophil rolling: microvillus elongation stabilizes P-selectin bond clusters. Biophys J. 2002;82:1835-1847.
71. Barsegov V, Thirumalai D. Dynamics of unbinding of cell adhesion molecules: transition from catch to slip bonds. Proc Natl Acad Sci U S A. 2005;102:1835-1839.
72. Finger EB, Puri KD, Alon R, Lawrence MB, von Andrian UH, Springer TA. Adhesion through L-selectin requires a threshold hydrodynamic shear. Nature. 1996;379:266-269.
73. Lawrence MB, Kansas GS, Kunkel EJ, Ley K. Threshold levels of fluid shear promote leukocyte adhesion through selectins (CD62L, P, E). J Cell Biol. 1997;136:717-727.
74. Lu H, Isralewitz B, Karmmer A, Vogel V, Schulten K. Unfolding of titin immunoglobulin domains by steered molecular dynamics simulation. Biophys J. 1998;75:662-671.
75. Gao M, Craig D, Vogel V, Schulten K. Identifying unfolding intermediates of FN-III_{10} by steered molecular dynamics. J Mol Biol. 2002;323:939-950.
76. Izrailev S, Stepaniants S, Balsera M, Oono Y, Schulten K. Molecular dynamics study of unbinding of the avidin-biotin complex. Biophys J. 1997;72:1568-1581.
77. Bayas MV, Schulten K, Leckband D. Forced detachment of the CD2-CD58 complex. Biophys J. 2003;84:2223-2233.

78. Bayas MV, Schulten K, Leckband D. Forced dissociation of the strand dimmer interface between C-Cadherin ectodomains. Mech Chem Biosys. 2004;1:101-111.
79. Lü SQ, Long M. Forced dissociation of selectin-ligand complexes using steered molecular dynamics simulation. Mol Cell Biomech. 2005;2:161-177.
80. Evans E, Berk D, Leung A. Detachment of agglutinin-bonded red blood cells. I. forces to rupture molecular-point attachments. Biophys J. 1991;59:838-848.